

EXPERIMENTAL STUDY ON STRENGTH AND DUCTILITY OF UNDERWATER FILLET WELDS IN REPAIRING OFFSHORE STEEL STRUCTURES

Xiao Chen¹, Yasuo Kitane¹ and Yoshito Itoh¹

ABSTRACT

Underwater wet welding is one of the most common repair measures for corroded offshore steel structures. Few studies have been carried out systematically concerned with mechanical properties of such welds, thus current design provisions rely heavily on limited experimental data on welds made underwater and design properties for corresponding welds made in air. This paper presents a series of experiments on forty-five fillet welded specimens featuring welding both in air and underwater. Weld strength and ductility of fillet welds are examined through strength tests, which are also complemented by Vickers hardness tests and microstructure examination to better understand the weld details. The tested parameters include two welding environments, two weld orientations, two base structural types, and four base steels. Based on the tests, differences between underwater and in-air fillet welds are examined in terms of strength, ductility, and failure modes, underwater weldability of base steels is also evaluated.

INTRODUCTION

Many offshore steel structures, including marine platforms, trestles, pier piles, etc. have been suffering from increasing corrosion damages. These corroded steel structures are in urgent need of repairing and strengthening to retain or extend their service lives. Among all repair strategies available, underwater wet welding is one of the most common measures due to its high efficiency and relatively low cost (Coastal Development Institute of Technology 1997, Liu 2005). This technique has been adopted over years and gained popularity in offshore and maritime engineering for recent energy explorations into the sea (Wernicke and Billingham 1998).

However, because of remarkable difference in welding environments, mechanical properties of welds produced underwater vary distinctly from those produced in air. Underwater welds have been studied a lot during past decades, most studies have focused on their metallurgical features (Kinugawa and Fukushima 1982, Ibarra et al. 1988), influence of quenching (Pope et al. 1996), development of new electrodes suitable for underwater wet welding (West et al. 1990), etc. Although some papers have studied mechanical properties of underwater welds (Akselsen et al. 2006, Zhang et al. 2003, Rowe et al. 2002), few studies have been carried out systematically for weld joint design. Due to a deficiency of test data, Japanese provision discounts strength of underwater welds by taking 80% of that of in-air welds irrespective of structural types, weld orientations, base steel types, and corrosion effects (Coastal Development Institute of Technology 1997). The main motivation of present study is to provide fundamental data on the strength of underwater fillet welds.

In this study, forty-five fillet welded specimens are tested to failure. Weld strength, ductility, and failure modes are examined with respect to two welding environments: in-air and underwater,

¹ Dept. of Civil Engineering, Nagoya University; Nagoya, Japan

two structural types: steel pipe and steel sheet pile, two weld orientations: transverse and longitudinal, and four base steels commonly used in offshore structures: SY295, SYW295, and corroded SY295 for steel sheet piles, and STK400 for steel pipes. SY295, SYW295, and STK400 are Japanese Industrial Standard (JIS) designations, and they are specified in JIS A5528, JIS A5523, and JIS G3444, with defined yield stresses 295 MPa, 295 MPa, and 235 MPa, respectively. Differences in mechanical properties between underwater welds and their counterpart in-air welds are investigated qualitatively as well as quantitatively. To understand weld features in detail, Vickers hardness tests and microstructure examinations are also performed to corroborate the mechanical features of underwater fillet welds. Based on experimental results, the paper ends with conclusions on weld strength and ductility in various cases.

EXPERIMENT PROGRAM

The main variables investigated in the fillet weld tests are welding environments, structural types, weld orientations, and base steel types. Table 1 presents the test matrix indicating different weld assemblies with their designations and parameters.

Test Specimens and Material Properties

Two configurations of specimens with different weld orientations are illustrated schematically in Fig. 1. In order for welds to fail before base or cover steels yield, the weld leg length is specified

Table 1. Test matrix

Assembly Designation	No. of Specimens	Structural type	Welding environment	Weld orientation	Base steel	Base thickness(mm)	Weld length(mm)	Cover steel
1	TYA	Sheet pile	In air	Transverse	SY295	12.7 mm	40 mm	SM490A
2	TWA				SYW295			
3	LYA			SY295				
4	LWA			Longitudinal	SYW295			
5	LCA				CSY295			
6	TYW		Underwater	Transverse	SY295	12.7 mm	40 mm	
7	TWW				SYW294			
8	LYW			SY295				
9	LWW			Longitudinal	SYW295			
10	LCW				CSY295			
11	TSA	Pipe*	In air	Transverse	STK400	12.7 mm	40 mm	SM490B
12	LSA			Longitudinal				
13	TSW		Underwater	Transverse				
14	LSW			Longitudinal				

*Test data for pipe are from Watanabe et al. (2009).

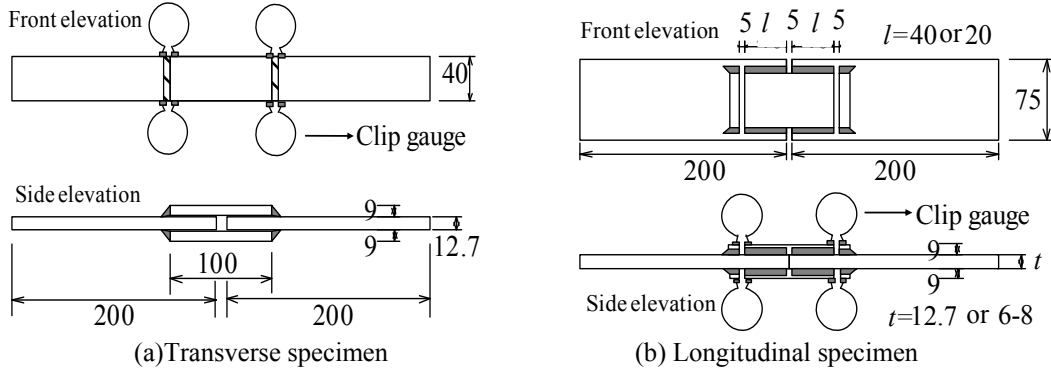


Fig. 1. Specimen configurations (in mm)

as 6 mm. One weld pass is used in welding process for all welds. Other welding details are listed in Table 2. Mechanical properties of steels, listed together with chemical compositions in Table 3, are obtained from static tensile coupon tests. To distinguish corroded and uncorroded SY295 steels, corroded SY295 base steels is referred to as CSY295 in this paper. It should be noted that CSY295 base plates with thickness varying from 6 to 8 mm are cut from in-situ steel sheet piles, which have been exposed to marine environment for about 35 years, to study corrosion effects on weld properties. Before tests, accurate weld profiles are measured by a laser displacement sensor.

Table 2. Welding details

Case	Welding environment	Orientation	Current(A)	Voltage(V)	Welding Velocity (mm/min)	Temperature (°C)	pH	Salinity (wt-%)
Sheet pile	In air	Longitudinal	70-80	12-16	65-85	17	-	-
		Transverse	55-70	10-20	145-200			
	Underwater	Longitudinal	80-95	19-23	60-70	14	7.9	2.6
		Transverse	75-95	16-23	120-160			
Pipe	In air	Longitudinal	100-110	20-30	79	-	-	-
		Transverse	90-100	20-40	88			
	Underwater	Longitudinal	120-140	20-40	79	25.6	8.2	2.1
		Transverse	120-140	20-40	88			

Test Setup

The specimens are tested quasi-statically under monotonic tensile loading using a 500 kN MTS material testing machine. Deformation of individual weld is recorded during the test by clip gauges placed at the ends of welds shown in Fig.1. Fig. 2 illustrates test setup in the experiment program. In this study, weld strength is defined as

$$\sigma_w = \frac{P_{\max}}{n\bar{a}l} \quad (1)$$

where σ_w is the fillet weld strength, P_{\max} is the maximum load of the specimen, \bar{a} is the average throat thickness of all welds in concerned specimen, l is the average weld length, n is the number of welds in specimen's cross section, which is 2 for transverse specimens, 4 for longitudinal specimens. By adopting n , the formula implicitly assumes the total load is shared equally by welds in the same cross section of specimen in spite of slight asymmetry in the weld shape. Weld ductility, a normalized deformation factor, is defined as

$$\Delta l = \frac{\Delta_f}{s} \quad (2)$$

where Δl is ductility factor, Δ_f is fracture deformation of the first fractured weld, and s is weld size. The definition of weld size is shown in Fig. 3.

Table 3. Material properties of steels

Material	Mechanical properties					Chemical compositions (wt-%)					
	Young's modulus, E(GPa)	Poisson's ratio, ν	Yield stress, σ_y (MPa)	Ultimate stress, σ_u (MPa)	Elongation, $\Delta\ell$ (%)	C	Si	Mn	P	S	CE _{IW} *
SY295	213	0.29	273	497	41	0.30	0.06	0.72	0.016	0.020	0.430
CSY295	212	0.29	349	531	34	0.27	0.02	0.96	0.013	0.019	0.433
SYW295	213	0.28	392	513	42	0.10	0.23	1.41	0.020	0.005	0.379
STK400	203	0.28	362	394	41	0.12	0.10	0.56	0.013	0.006	0.230
SM490A	209	0.28	361	532	39	0.16	0.34	1.44	0.015	0.007	0.457
SM490B	213	0.28	290	416	46	0.12	0.23	1.02	0.013	0.003	0.328
Electrode **	-	-	410	460	30	0.10	0.10	0.43	0.015	0.007	0.188

* CE_{IW} = C+(Si+Mn)/6+(Cr+Mo+V)/5+(Ni+Cu)/15. Only first two terms used except SYW295.

**Catalogue value from the manufacturer.

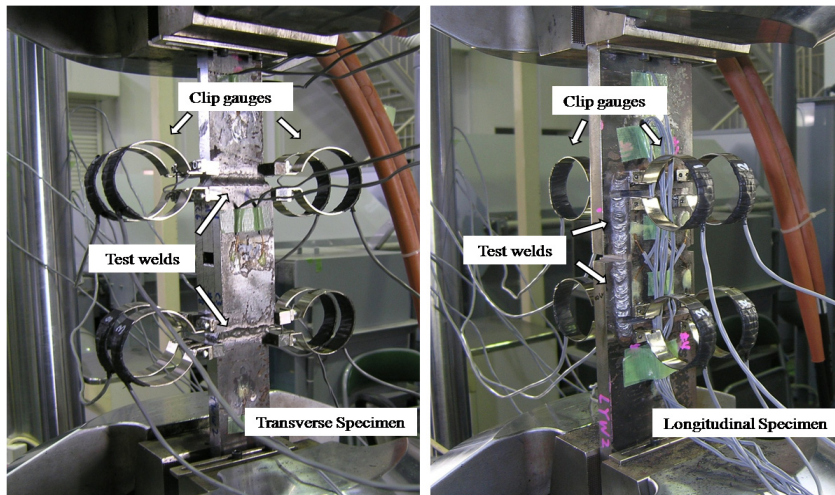


Fig. 2. Test setup

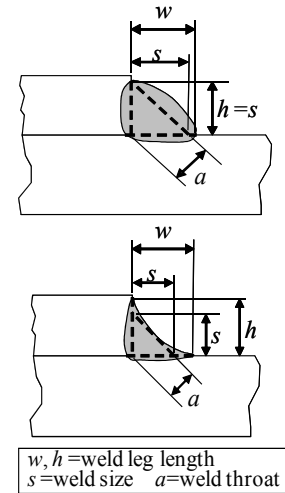


Fig. 3. Definition of weld sizes

EXPERIMENTAL RESULTS AND DISCUSSIONS

Load-Deformation Curves

Generally, welds on the specimens of the same assembly exhibit similar load-deformation responses, even for the welds located on either convex or concave side of pipe material STK400. In order to compare results clearly, 14 load-deformation curves of the first failed weld, one of each assembly type, are plotted in Fig. 4. Depending on the size of weld throat, stiffness during

initial elastic phase varies from 1738 to 2761 kN/mm. Most of underwater welds show larger ultimate load when compared with their counterpart in-air welds. However, due to the significantly smaller weld throat, LSW specimen with an average weld throat 3.7 mm has a smaller ultimate load than LSA specimen with an average weld throat 5.0 mm. Another observation is that all underwater weld specimens show significantly smaller fracture deformation than their counterpart in-air welds. There are always “plateau” before in-air welds fail, while for underwater welds, fracture comes soon after their maximum loads.

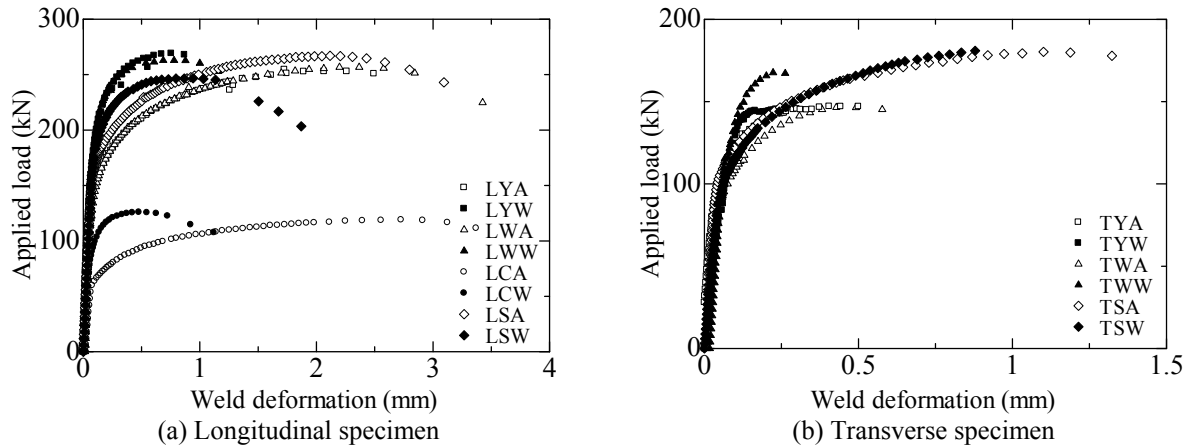


Fig. 4. Load-deformation curves of welds

Strength and Ductility

To examine the results quantitatively, weld strength versus ductility factor are plotted in Fig. 5. In general, underwater welds show higher strength but lower ductility than in-air welds although some differences exist among different weld assemblies. Fig. 6 shows strength increase and ductility decrease of underwater welds in percent when compared with counterpart in-air welds. Strength increase ranges from 6.9% to 41.0%, while ductility decrease is about 50% except two cases: transverse welds on SY295 and longitudinal welds on CSY295. Moreover, weld orientations affect this strength increase and ductility decrease due to underwater welding to some degree as observed in Fig. 6. As for welds on SY295, strength increase is nearly doubled from 23.7% to 41.0% and ductility decrease is also nearly doubled from 23.8% to 50.3% when weld orientations change from the transverse to the longitudinal, although those of SYW295 are not affected. Welds on corroded SY295 exhibit a relatively small strength increase of 21.7% but a drastic ductility decrease of 88.1%. As for absolute values, the LCA welds have the largest ductility factor with an average value of 0.61 but their counterpart underwater welds, LCW, have the smallest ductility factor with an average value of 0.09 among all longitudinal welds.

It should also be noted that the strength of longitudinal welds tends to increase with ductility factor as shown in Fig. 5(a), and this trend is more pronounced in welds produced underwater. It is found that weld strength, to some extent, is affected by how much the weld can deform before its failure. Regarding nonuniform stress distribution in longitudinal fillet welds, where the shear stress is larger at two ends and smaller in between (Suzuki 1982), smaller ductility will prevent additional load from being shared by weld elements in the central region after weld elements at the two ends yield. Consequently, the smaller the deformation capacity at weld ends in a longitudinal weld, the smaller weld strength will be. As expected, no positive correlation between strength and ductility is found in transverse welds made underwater or in-air as shown in Fig. 5(b), as a result of the uniform distribution of shear stress in the weld beads.

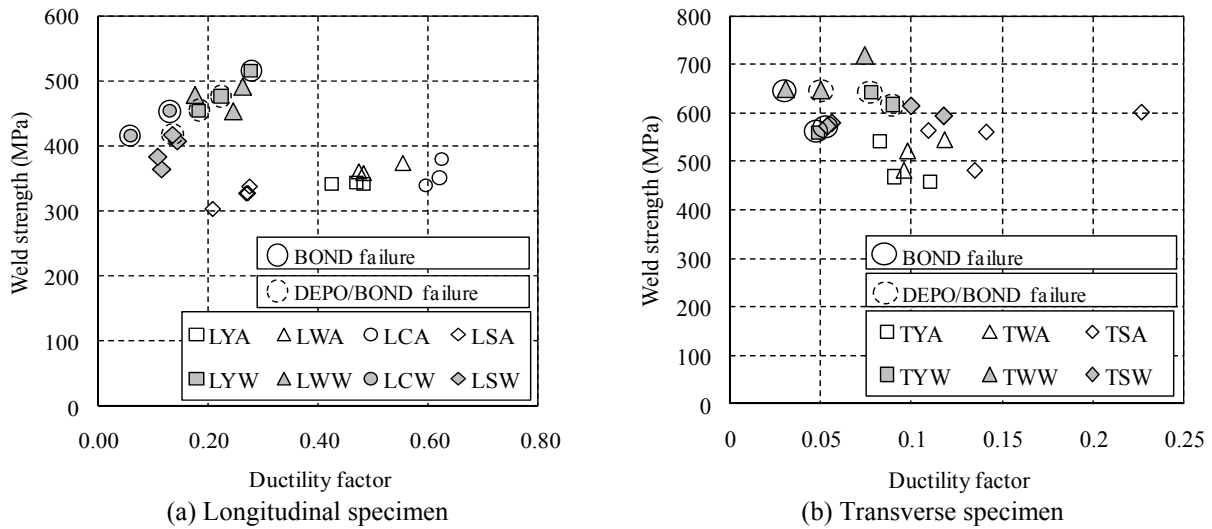


Fig. 5. Weld strength versus ductility factor

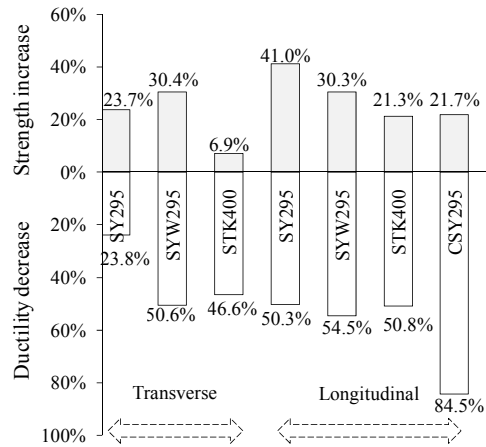


Fig. 6. Relative change of weld strength and ductility of underwater welds when compared with in-air welds

To examine the effect of corrosion on strength and ductility of fillet welds, welds on corroded SY295, i.e. CSY295, and those on SY295 are compared. Although the chemical compositions of CSY295 and SY295 are similar as shown in Table 3, LCW welds with an average strength of 435 MPa exhibit smaller strength by 10.8% than LYW welds with an average strength of 482 MPa. However, for corresponding in-air welds, LCA welds have slightly larger strength with an average strength of 357 MPa than LYA welds with an average strength of 342 MPa. This phenomenon can be explained by ductility of those welds. LCW welds show a ductility factor of 0.09, while LYW welds show 0.23 which is 2.6 times larger than LCW. As for LCA and LYA welds, the ductility factors are 0.61 and 0.46, respectively. The smaller ductility of LYA results in the smaller strength than LCA welds. The ductility factor of LCW is turned out to be the smallest among all longitudinal welds, which will be examined in the following sections of failure modes and hardness distribution.

Failure Modes

In Fig. 5, the failure modes are also indicated. It is observed that specimens failed at weld deposit (DEPO) except for those circled welds which fail either at boundary between weld deposit and base metal (BOND) or with a combination of DEPO and BOND (DEPO/BOND). Fig. 7 shows representative photos of different failure modes. It is of interest to note that BOND and DEPO/BOND failure modes occurred only in underwater welds. All six underwater fillet welds with base steel SY295 fail at BOND or DEPO/BOND regardless of the weld orientations, and all two underwater fillet welds with base steel CSY295 exhibit brittle fractures at BOND, with little deformation in weld metals, consequently lower ductility and smaller strength are inevitable in LCW welds. Moreover, with base steels of STK400 and SYW295, underwater fillet welds fail at BOND or DEPO/BOND with frequencies of two out of eight and two out of six respectively. Considering the differences in carbon contents of base steels as shown in Table 3, the findings in failure modes suggest that “milder” steels STK400 and SYW295 with lower carbon equivalents of 0.230 and 0.379, respectively, have better weldability in underwater environments than “tougher” steels SY295 and CSY295 with higher carbon equivalents of 0.430 and 0.433, respectively.

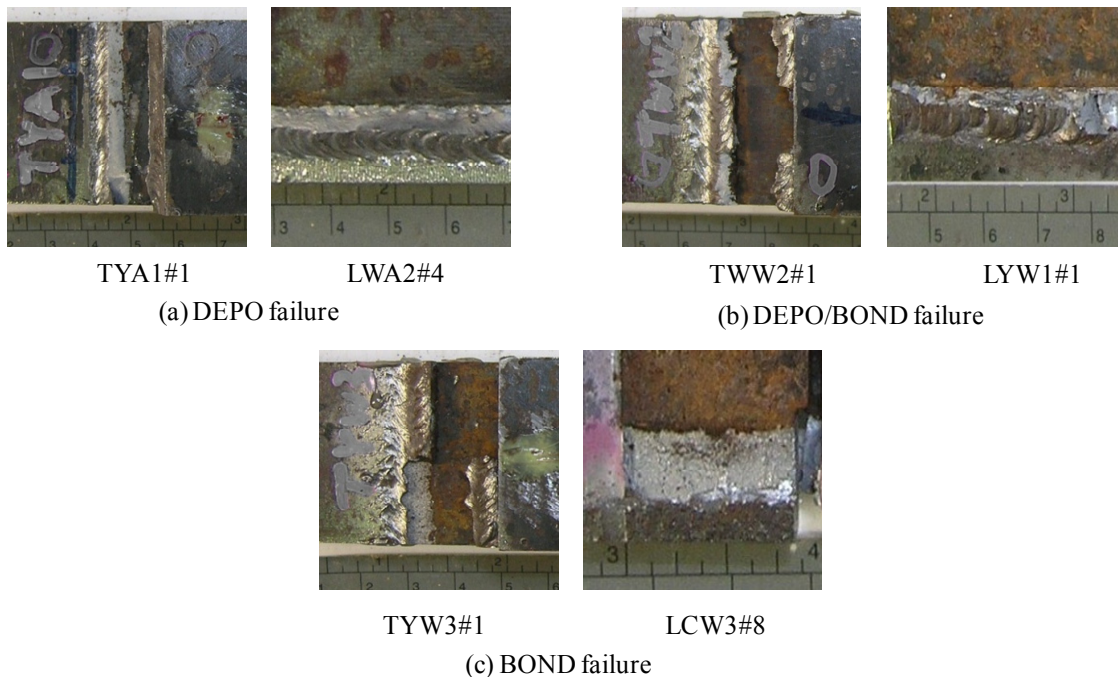


Fig. 7. Comparison in failure modes

Hardness and Microstructures

Welding is a thermo-mechanical process, and weld properties are closely related to thermal conditions which dominate weld microstructures and in turn affect mechanical properties. This section discusses results from Vickers hardness tests and metallographic examinations of fillet welds. The specimens for hardness tests are produced simultaneously with specimens for weld strength tests to ensure the same welding conditions.

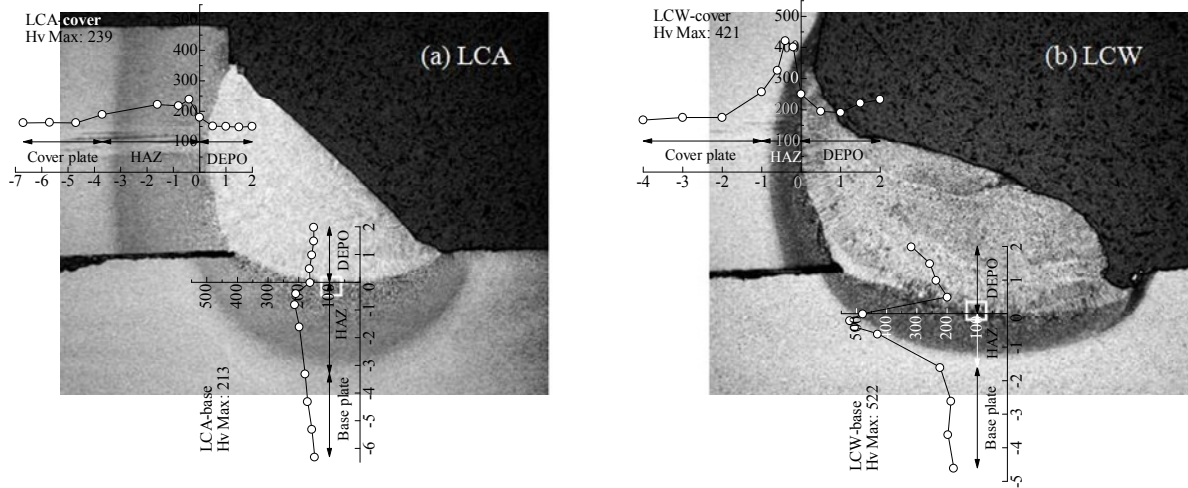


Fig. 8. Hardness distribution of welds

Fig. 8 shows photos of polished and etched cross sections of LCA and LCW specimens with Vickers hardness results superimposed. Points for hardness data acquisition are located along the arrows. Two small windows in white at boundaries of weld deposit and heat affected zone (HAZ) signify the areas where microstructure images shown in Fig. 9 are taken. These photos are representative to reveal general features of fillet welds examined in this study, although there are some differences in the magnitude of hardness and detailed microstructures among different weld assemblies. As shown in Fig. 8, hardness peaks can be found in the coarse grained region of HAZ in both in-air and underwater welds. Due to the rapid quenching, heat transfer is limited in a smaller region resulting a HAZ size of 1 to 2 mm and HAZ hardness of 310 to 526 Hv for underwater welds whereas they are 3 to 4 mm and 198 to 375 Hv for in-air welds.

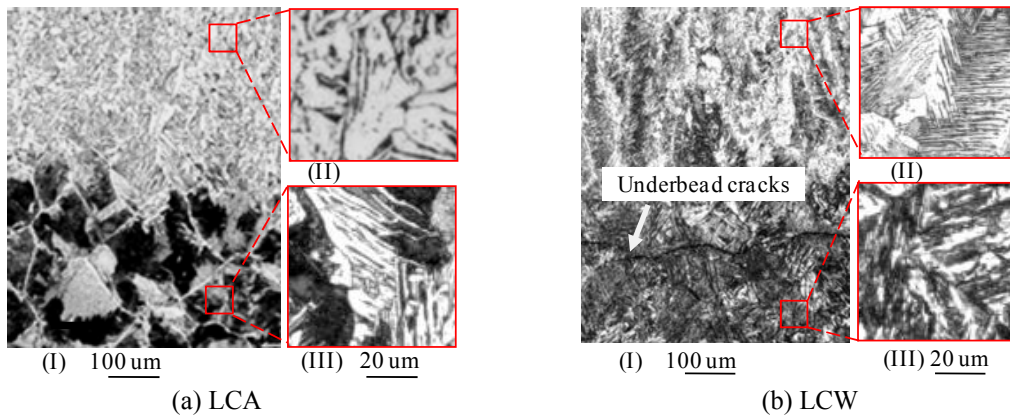


Fig. 9. Weld microstructures at the boundary of DEPO and HAZ

Moreover, there are similar tendencies of microstructure distributions within welds made in the same environment despite of differences in base steels. Microstructures of LCA and LCW welds at BOND areas are illustrated in Fig. 8a(I) and 8b(I). The microstructures of DEPO are shown in Fig. 8a(II) and 8b(II), DEPO in LCA is mainly composed of ferrite and pearlite with 150 Hv and DEPO in LCW is composed of ferrite-pearlite jointly with 170 Hv. The microstructures at HAZ in LCA, as shown in Fig. 8a(III), are composed of ferrite and pearlite with 200 Hv, while the microstructures at HAZ in LCW, as shown in Fig. 8b(III), are dominated by martensite with 500 Hv. In addition, there are underbead cracks found in the boundary areas between DEPO and

HAZ only in, but not all underwater welds. Underbead cracks are observed in the boundary areas in TYW, LYW welds, and more in LCW welds, these welds are on SY295 and CSY295 steels. Whereas no crack is observed in TWW, LWW, TSW and LSW welds on SYW295 and STK400 steels, although some of them exhibit BOND failures. This further corroborates that SY295 steels do not have good weldability in the underwater wet environment although they are quite sound in the open air environment compared with SYW295 and STK400 steels. The distinct mechanical mismatching and many underbead cracks in the boundary areas between DEPO and HAZ are responsible for the significantly low ductility of LCW welds.

CONCLUSIONS

Underwater fillet welds were studied experimentally with respect to strength and ductility. Fourteen fillet weld assemblies, 45 specimens in total, were tested to failure. Mechanical properties of underwater welds were examined when compared with their counterpart in-air welds. Main conclusions obtained in this study are summarized below.

1. Underwater fillet welds have larger strength but smaller ductility when compared with in-air welds. Strength increase of underwater welds when compared with their counterpart in-air welds ranges from 6.9% to 41.0% depending on weld assemblies, while ductility decrease is nearly the same at 50%.
2. When the weld orientation changes from the transverse to the longitudinal direction, the strength increase is nearly doubled from 23.7% to 41.0% on SY295 steels, tripled from 6.9% to 21.3% on STK400 steels and unchanged at around 30% on SYW295 steels. Underwater longitudinal welds exhibit a pronounced positive correlation between weld strength and ductility factor.
3. Underwater fillet welds on corroded SY295 steels show a strength increase of 21.7% and a drastic ductility decrease of 84.5% when compared with those on original SY295 steels. This inferior ductility is found to be caused by mechanical mismatching and underbead cracks in the boundary areas between DEPO and HAZ.
4. The weldability of STK400 and SYW295 steels is good in both in-air welding and underwater welding, while the weldability of SY295 steels, although it is quite sound in in-air welding, is undesirable in underwater welding.

ACKNOWLEDGMENTS

This research was partially supported by The Japan Iron and Steel Federation and Nagoya University. The authors would like to acknowledge their support.

REFERENCES

- Akselsen, O. M., Fostervoll, H., Harsvaer, A., Aune, R. 2006. Weld metal mechanical properties in hyperbaric GTAW of X70 pipeline. *International Journal of Offshore and Polar Engineering* **16**(3):233-240.
- Coastal Development of Institute of Technology. 1997. *Port Steel Structure Corrosion-Prevention and Repair Manual*. Coastal Development Institute of Technology, Japan (in Japanese).
- Ibarra, S., Grubbs, C. E., and Olson, D.L. 1988. Metallurgical aspects of underwater welding. *Journal of Metals* **40**(12):8-10.

- Kinugawa, J., and Fukushima, S. 1982. Influence of equivalent carbon contents of steels on proportions of martensite, hardness and susceptibility to cold cracking at coarse-grained regions in underwater wet welding. *Welding Society Journal* **51**(3):45-51 (in Japanese).
- Liu, S. 2005. Maintenance and repair welding in the open sea. *Welding Journal* **84**(11):54-59.
- Pope, A., Teixeira, J., Dos Santos, V., Paes, M., and Liu, S. 1996. The effect of nickel on the mechanical properties of high-oxygen underwater wet welds. *Journal of Offshore Mechanics and Arctic Engineering Transactions of the ASME* **118**(2):165-168.
- Rowe, M. D., Liu, S., and Reynolds, T. J. 2002. The effect of Ferro-Alloy additions and depth on the quality of underwater wet welds. *Welding Journal* **81**(8):156S-166S.
- Suzuki, H. 1982. *Recent Welding Engineering*. Corona Publishing Co., Ltd. Tokyo, Japan (in Japanese).
- Watanabe, N., Kitane, Y., and Itoh, Y. 2009. Modeling of joint behavior of steel pipes repaired with steel plate by underwater wet welding. *Journal of Structural Engineering, JSCE* **55A**(3):903-914 (in Japanese).
- Wernicke, R., and Billingham, J. 1998. Underwater wet repair welding and strength testing on pipe-patch joints. *Journal of Offshore Mechanics and Arctic Engineering, ASME* **120**(4):237-242.
- West, T. C., Mitchell, G., and Lindberg, E. 1990. Wet welding electrode evaluation for ship repair. *Welding Journal* **69**(8):46-56.
- Zhang, X. D., Chen, W. Z., Ashida, E., Matsuda, F. 2003. Metallurgical and mechanical properties of underwater laser welds of stainless steel. *Journal of Material Science & Technology* **19**(5):479-483.